(73) Beightler, C. S.; Phillips, D. T.; Wilde, D. J. *Foundations of Optimization*, 2nd ed.; Prentice-Hall: Engelwood Cliffs, NJ, 1979.
(74) Marquardt, D. W. *SIAM J. Appl. Math.* **1963**, *11*, 431.
(75) Birkhoff, G.; Mac Lane, S. M. *A Survey of Modern Algebra*, 3rd ed.; Macmillan: New York, 1965.
(76) Wang, Z.-L.; Wang, Q.-W.; Fetters, L.; Chu, B. In *Proceedings of the Chemistry International Symposium on New Trends in Physics and Physical Chemistry of Polymers Honoring Professor P. G. de Gennes*, in press.
(77) Chu, B.; Xu, R.-L.; Nyeo, S.-L. *Part. & Part. Syst. Charact.* **1989**, *6*, 34.

Formation and Torsion Dynamics of the Stereocomplex of Isotactic and Syndiotactic Poly(methyl methacrylates) Studied by the Fluorescence Depolarization Method

Takashi Sasaki and Masahide Yamamoto*

Department of Polymer Chemistry, Kyoto University, Kyoto 606, Japan.
Received November 2, 1988; Revised Manuscript Received March 15, 1989

ABSTRACT: The dynamics of the stereocomplex of poly(methyl methacrylate) (PMMA) was studied by the fluorescence depolarization method. Anthracene-labeled syndiotactic PMMA was mixed with isotactic PMMA in toluene dilute solutions to form the anthracene-labeled stereocomplex. The formation of the stereocomplex was followed over the period of 3 weeks by the steady-state measurement. The stoichiometry of the complex formation was revealed to be isotactic/syndiotactic = 1/2 for this system. Time-resolved fluorescence emission anisotropy data, $r(t)$, were well explained by the intermediate zone formula of the torsion dynamics theory for stiff macromolecules. This fact supports the idea of the double-stranded helical structure for the stereocomplex. The torsional rigidity of the stereocomplex under the gel structure was estimated from $r(t)$ to be $\alpha = 2.4 \times 10^{-10}$ dyn cm and $C = 6.0 \times 10^{-18}$ dyn cm^2 at 25 °C, which are values larger than those obtained for DNA.

I. Introduction

Isotactic and syndiotactic stereoregular poly(methyl methacrylates) (i-PMMA and s-PMMA) associate in certain proper solvents, in a so-called stereocomplex.[1-3] The complexation occurs at the weight ratio of i-PMMA/s-PMMA = 1/2 in certain solvents.[4] The association is said to be caused by nonbonded interactions of CH_3 groups and ester groups.[5] Recent investigations on this phenomenon have revealed the structure and the complexation mechanism to some extent.[6-8] Also the stereospecific polymerization of methyl methacrylate (MMA) in the presence of stereoregular PMMA as a template is closely related to the stereocomplex formation.[9,10] Recently, the mechanical properties of the PMMA stereocomplex have been studied as an application.[11]

Bosscher et al.[7] investigated the structure of the stereocomplex of i-PMMA and s-PMMA by X-ray diffraction and by conformational energy calculations. Their results revealed a double-stranded helical structure consisting of an isotactic 30/4 helix surrounded by a syndiotactic 60/4 helix, with a real fiber period of 73.6 Å. The structure is illustrated by contours of i-PMMA and s-PMMA in Figure 1. The helical pitch is 18.4 Å, which corresponds to 7.5 monomer units of i-PMMA and 15 monomer units of s-PMMA. In this structure, one monomer unit of i-PMMA meets two monomer units of s-PMMA, and this idea is consistent with the weight ratio of the stereocomplex that i-PMMA/s-PMMA = 1/2. The dynamic behavior in solutions of the stereocomplex of such a helical structure may resemble that of a double-stranded helix of DNA rather than that of synthetic flexible polymer chains. However, no investigations on the dynamics of the PMMA stereocomplex have been done so far.

The fluorescence method was utilized to investigate the formation of other polymer complexes. Morawetz and his co-workers[12,13] investigated the kinetics of the complex formation of poly(acrylic acid) (PAA) and poly(oxyethylene) (POE) by detecting the fluorescence intensity of the dansyl group attached to the PAA chain. Anufrieva et al.[14] examined the exchange of the components of the PAA–POE complex by the fluorescence depolarization method. Uchida[15] also investigated the complexation of stereoregular PMMA, which was labeled with perylene, by the steady-state measurement of fluorescence depolarization. In general, the fluorescence depolarization measurement provides the information of local mobility, and this method is expected to be fairly sensitive to the complexation phenomenon, which is associated with drastic changes in the local environment.

As for the dynamics of rigid macromolecules such as DNA, theoretical treatment of a deformable filament model of twisting and bending has been developed,[16,17] and it has become possible to investigate the torsion dynamics of DNA from experimental data of fluorescence polarization anisotropy,[18,19] electric birefringence,[20,21] and transient photodichroism.[22] In the time region within 100 ns, the relaxation phenomena are mainly attributed to the torsional (twisting) motions in the case of a sufficiently long chain. The theory also treats internal relaxations such as libration or wobbling of the intercalated dye in a very rapid time region as in the picosecond fluorescence depolarization experiments.

In the present work, we investigated the formation and dynamics of the stereocomplex of isotactic and syndiotactic PMMAs in toluene solutions by the fluorescence depolarization method in the nanosecond time region. For this purpose, s-PMMA labeled with the anthracene group in the middle of the chain was mixed with unlabeled i-PMMA in dilute toluene solutions to form the anthracene-labeled stereocomplex filament. The labeled s-PMMA has also been used to investigate the local conformational motions in dilute solutions,[23] and the transition vector of the anthracene label lies parallel to the backbone of the s-PMMA chain. The theory of torsion dynamics was applied to the

0024-9297/89/2222-4009$01.50/0

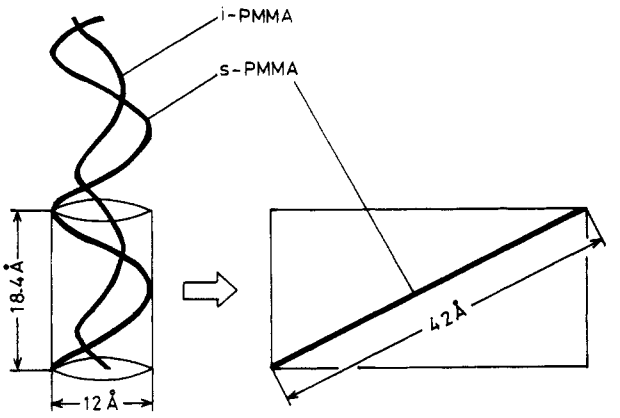

Figure 1. Double-stranded helical structure of the PMMA stereocomplex and estimation of the equilibrium polar angle of the transition dipole, ϵ_0. The transition dipole of the anthracene label lies along the contour of the s-PMMA chain. The s-PMMA chain takes the helical structure of 60/4 with a real fiber period of 73.6 Å;[7] i.e., a helical filament of 18.4 Å is made up of 15 monomer units of the s-PMMA. Assuming that the contour length of the s-PMMA of 15 monomer units is 42 Å, we obtain $\epsilon_0 = 64°$.

data, and we estimated the torsional rigidity of the stereocomplex and compared it with that of DNA.

II. Formula of the Fluorescence Emission Anisotropy of the Twisting Stereocomplex

The formulas of time-resolved fluorescence emission anisotropy for filamentous macromolecules of twisting and bending were proposed by Barkley and Zimm[16] and also by Allison and Schurr.[17] Later, Schurr[24] pointed out deficiency in the formula by Barkley and Zimm and reconstructed the expression for the fluorescence anisotropy in terms of twisting, bending (tumbling), and internal (wobbling) correlation functions. According to the theory, the general expression for the fluorescence anisotropy ratio can be written as

$$r(t) = r_0 \sum_{n=0}^{2} W_n(t)\ C_n(t)\ F_n(t) \tag{1}$$

where r_0 is the initial anisotropy ratio, $W_n(t)$ the internal correlation function, $C_n(t)$ the twisting correlation function, and $F_n(t)$ the bending correlation function.

The internal correlation function $W_n(t)$ describes the wobbling motion of the intercalated dye in the DNA fragment. In our case, the anthracene label is rigidly attached to the syndiotactic chain, so that the amplitude of the wobbling motion may be relatively small compared to the intercalated dyes. At certain longer time (usually in the nanosecond time region), when the wobbling correlation has completely relaxed, the internal correlation function becomes independent of time. Assuming that the absorption dipole of the anthracene label is parallel to the emission dipole, the internal correlation function is expressed as

$$W_0 = (3/2 \cos^2 \epsilon_0 - 1/2)^2 \tag{2}$$

$$W_1 = 3 \cos^2 \epsilon_0 \sin^2 \epsilon_0 \tag{3}$$

$$W_2 = 3/4 \sin^4 \epsilon_0 \tag{4}$$

where ϵ_0 is the equilibrium polar angle of the transition dipole, i.e., the angle between the helix axis and the transition dipole. In the present case, the transition dipole lies parallel to the contour of s-PMMA. According to Bosscher et al., the distance 18.4 Å along the helix axis of the stereocomplex corresponds to 15 monomer units of the s-PMMA.[7] The corresponding contour length of the s-PMMA can be estimated from the shift factor M_L of the helical wormlike chain model established by Yamakawa and his co-workers, which means the molecular weight per unit contour length.[25] We employed $M_L = 35.7$ Å^{-1} for s-PMMA.[26] The contour length of 15 monomer units we obtained was 42.0 Å. From this value, we can estimate ϵ_0 to be 64° (Figure 1), and then $W_0 = 0.0448$, $W_1 = 0.4657$, and $W_2 = 0.4894$.

Table I
Molecular Weights and Triad Tacticity of the Polymers Used in This Study

	$M_n \times 10^{-4}$	$M_w \times 10^{-4}$	tacticity, % I	H	S
s-PMMA labeled	12.8	15.0	0	14	86
s-PMMA unlabeled	6.58	8.25	0	14	86
i-PMMA	1.04	1.62	100	0	0

The twisting correlation function $C_n(t)$ can be expressed by a series of accurate analytical formulas with respect to five time zones.[24] Here, we employ the formula for the intermediate zone, which is expressed as

$$C_n(t) = \exp[-n^2 k_B T (t/\pi\alpha\gamma)^{1/2}] \tag{5}$$

where k_B is the Boltzmann constant, α the torsional rigidity per a subunit rod (or between rods), and γ the friction factor for rotation of a subunit rod about its helix axis. In the intermediate zone, the higher order normal relaxation modes play a role, and the effect of the length of the fragment is negligible. The intermediate zone often lies in the time range of 10^{-8}–10^{-9} s, and in such a case, the fluorescence depolarization becomes a powerful tool.

The formula of the bending correlation function $F_n(t)$ has been derived theoretically by Barkley and Zimm.[16] On the other hand, an empirical formula derived from the electric birefringence experiment provides reasonable analysis of the data for DNA.[27] In the present case, we assume $F_n(t) = 1.0$, namely the helix axis is immobile within the time span of our experiment (the fluorescence lifetime of the anthracene label is about 8.5 ns in the present study). The stereocomplex formation in our experiment was usually associated with the gelation. This suggests a network structure in the solution; i.e., each polymer chain may occasionally associate with more than one polymer chain leading to cross-linking. In such a case, the bending motions are strongly inhibited, and the twisting motions in the local domain are mainly detected by the nanosecond time-resolving measurement of fluorescence depolarization. Also the formula of $C_n(t)$ in the intermediate time zone, which is independent of the number of rods (chain length or molecular weight), seems to be appropriate for the present system.

Finally, the formula of the time-dependent anisotropy ratio used to analyze the data for the stereocomplex becomes

$$r(t) = r_0\{0.045 + 0.466 \exp[-t^{1/2}/b] + 0.489 \exp[-4t^{1/2}/b]\} \tag{6}$$

with

$$b = (\pi\alpha\gamma)^{1/2}/k_B T \tag{7}$$

III. Experimental Section

The s-PMMA labeled with anthracene in the middle of the polymer chain was prepared as described previously.[23] The unlabeled s-PMMA was also prepared by anionic polymerization with (1,1-diphenyl-3-methylpentyl)lithium in THF at −78 °C. The unlabeled i-PMMA was prepared by anionic polymerization with *tert*-C_4H_9MgBr in toluene at −78 °C.[28] Table I shows the molecular weights and the triad tacticity of these polymers determined by GPC and ^{13}C NMR, respectively.

Table II
Contents of the Sample Solutions

sample no.	s-PMMA, wt %	i-PMMA, wt %	$f_{i/t}$
1	2.74	0.26	0.087
2	2.47	0.53	0.177
3	2.11	0.89	0.297
4	1.62	1.38	0.460
5	0.68	2.32	0.773

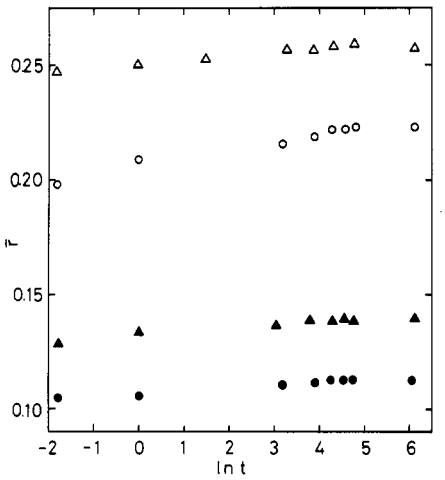

Figure 2. Changes of the averaged anisotropy ratio, $\bar{r}$, against logarithm of time (h) at 22 °C: (●) no. 1, (▲) no. 2, (○) no. 3, and (△) no. 5. The data for the sample no. 4 were almost the same as those for no. 5, so they are not shown here.

The complexation was observed in toluene with various mixing ratios of the isotactic and syndiotactic PMMAs (Table II). The value $f_{i/t}$ in Table II represents the weight fraction of i-PMMA to the total polymer quantity in each solution. The labeled s-PMMA was added so that the concentration of the anthracene group becomes 10^{-5} mol L^{-1}, and the total polymer concentration was made 3 wt % for all the samples by the addition of the unlabeled s-PMMA and i-PMMA. The mixed polymer solutions were heated at 70 °C until the solutions were completely homogeneous (for 10–30 min). Then, the sample solutions were cooled to room temperature (22 °C). This time was defined as the point of time zero. The change of the averaged (steady-state) anisotropy ratio, $\bar{r}$, was measured over the period of 3 weeks at 22 °C for each sample by a spectrophotometer Hitachi Model 850 equipped with polarizing HNP'B filters. After these measurements were completed, the time-resolved anisotropy ratio, $r(t)$, was measured for each sample at 25 °C by a nanosecond single-photon counting system in our laboratory.[23]

The time-resolved data were analyzed by the method of nonlinear least-squares fitting in order to obtain the best fit parameters for b and r_0 in eq 6. The detailed description of the fitting procedure is shown elsewhere.[23,29]

IV. Results and Discussion

Figure 2 shows the changes in the averaged fluorescence emission anisotropy $\bar{r}$ in the time span from 10 min to 3 weeks. We also measured the anisotropy ratio for the sample of $f_{i/t} = 0$ as reference ($t = 0$) and obtained that $\bar{r} = 0.085$. Thus, it is recognized that the anisotropy ratio increases very rapidly at the initial stage. Then, the averaged anisotropy ratio increases very slowly with time. This slow change may correspond to the increase in the number of anthracene labels that are in the complex-formed sites. The complex formation necessitates large-scale rearrangements of polymer chains, which take a relatively long time. After 5 days, the averaged anisotropy ratio became almost constant, so the samples were in their equilibrium states. Vorenkamp and Challa[30] proposed that the complex formation process consists of two steps, i.e., the formation of the compact particles (first step) and aggregation of the particles (second step). One may recognize the secondary rise (corresponding to the second step) of anisotropy ratio appearing near ln t = 4 (about 2 days). However, detailed discussion is not put forth here.

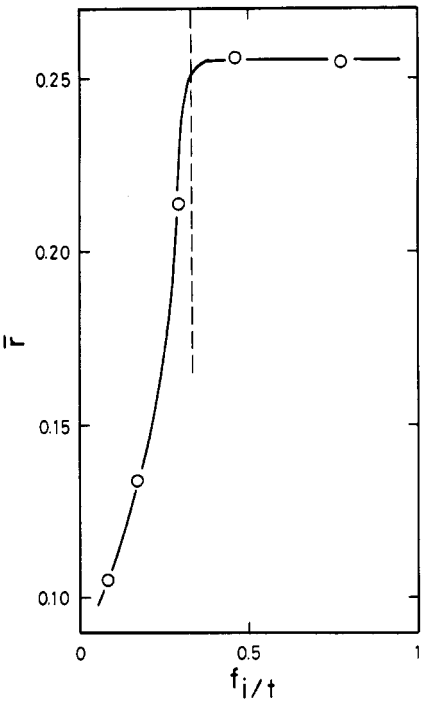

Figure 3. Plot of the averaged anisotropy ratio at the equilibrium state (after 3 weeks) against $f_{i/t}$, the weight fraction of i-PMMA to the total polymer quantity in the solution. The broken line represents the ideal value of $f_{i/t}$ (1/3).

The equilibrium values of the averaged anisotropy ratio are plotted against $f_{i/t}$, the weight fraction of the i-PMMA in Figure 3. The averaged anisotropy ratio increases with $f_{i/t}$ until $f_{i/t}$ reaches 1/3 (represented with a broken line in the figure), and above it, the anisotropy becomes constant (ca. 0.26).

Since the anthracene group is attached to the s-PMMA, nearly all the anthracene groups are in the complex-formed sites when $f_{i/t} > 1/3$ (i-PMMA/s-PMMA = 1/2). Thus, it is shown that the complexation occurs at the ratio of i-PMMA/s-PMMA = 1/2. However, note that the saturating point in Figure 3 is at a slightly larger value of $f_{i/t}$ than the ideal one (represented with the broken line). Even if the polymers are mixed just at the ideal ratio ($f_{i/t}$ = 1/3), some remnant syndiotactic segments, which cannot couple with isotactic segments, still exist, because the complex formation takes place randomly. Therefore, a slightly excess amount of isotactic fraction is necessary for all the syndiotactic segments to be coupled.

For the samples no. 3–5, gelation was observed within 10 min from the time zero point. This means that the stereocomplex formation occurs randomly along the polymer chains, and therefore, the chains are randomly cross-linked.

For the samples no. 1 and 2, no gelation was observed even after 3 weeks. In the present case, the molecular weight of the i-PMMA is lower than that of the s-PMMA and is rather low (see Table I). At high $f_{i/t}$'s, most of the s-PMMA (high molecular weight) is associated with the i-PMMA. Thus, the gelation may occur easily compared with those at lower $f_{i/t}$'s, where some of the long s-PMMA chains are not involved in the gelation.

Time-resolving measurements were executed for all the samples at the equilibrium states (after 3 weeks). The fluorescence intensity of the anthracene label decayed with the single-exponential term. The observed lifetimes are

Table III
Best Fit Parameters of the Twisting Correlation Function

sample no.	fluorescence lifetime, ns	r_0	b, ns$^{1/2}$	χ^2
4	8.5	0.278	71.1	1.336
5	8.6	0.279	62.9	1.035

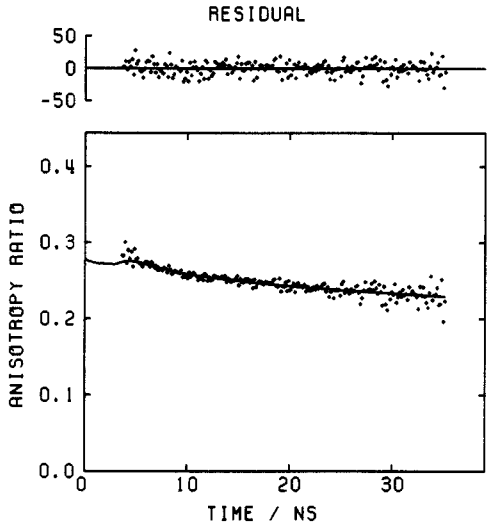

Figure 4. Anisotropy decay for the sample no. 5 at 25 °C. Dots represent experimental data, and the solid curve indicates the theoretical decay convoluted with the best fit parameters in Table III for the autocorrelation function of eq 6. The weighted residuals are also plotted on an arbitrary scale.

shown in Table III. The feature of $r(t)$ was quite different from that of s-PMMA in dilute solutions.[23] The formula of eq 6 was fitted to the observed anisotropy ratio $r(t)$, r_0, and b being treated as variable parameters. For the samples no. 1–3, the agreements are not good, because they contain the anthracene groups in the free sites. Indeed, the orientations of these anthracene groups are affected by the local conformational rearrangements (transitions), so the twisting model is not appropriate. For the samples no. 4 and 5, the agreements are sufficiently good in spite of the two-parameter fit as shown in Table III. The value of χ^2, which denotes the reduced sum of the squares of the residuals, is almost equal to 1. Figure 4 shows the fitted decay curve for the sample no. 5, which also shows a good agreement. Thus, we can say that the twisting model described in section II seems to be valid for our stereocomplex of PMMA. Equation 6 contains the assumption that the helix axis is immobile within our experimental time scale. In the present system, probably the orientational rearrangement of the helix axis is strongly hindered by the cross-linked points in the network structure, and also the chain length (the number of rods) may not affect the torsional motions. Hence, the twisting correlation function of eq 5, which is for the intermediate zone, shows good agreements for the samples no. 4 and 5. The above result certainly supports the idea of the double-stranded helical structure for the stereocomplex of PMMA.

Then, we estimated the torsional rigidity (torsion constant) α of the stereocomplex of PMMA. As is readily seen from eq 7, α is not determined independently from b. Therefore, we have to evaluate the friction factor γ by calculation. If we employ the sticking boundary condition, γ can be written as[31]

$$\gamma = 4\pi\eta a^2 hp \tag{8}$$

where η is the viscosity of the medium, a the hydrodynamic radius of the rod, h the height of the rod, and p the number of base pairs per a rod. Here, we employed the value η = 0.550 cP (25 °C), a = 7.2 Å, h = 18.4 Å/7.5 = 2.45 Å, and p = 1, so we obtained that $\gamma = 8.78 \times 10^{-24}$ dyn cm s (25 °C). In this case, the subunit rod consists of one monomer unit of i-PMMA and two monomer units of s-PMMA. Then, we obtained the torsional rigidity of the sample no. 5 as $\alpha = 2.4 \times 10^{-10}$ dyn cm at 25 °C by use of eq 7. Another torsional rigidity C, defined as $C = h\alpha$, was found to be 6.0×10^{-18} dyn cm^2.

Recently, much discussion has been done about the value of the torsion constant of DNA, and it is interesting to compare our results with those obtained on DNA, though the present torsional rigidity of the stereocomplex was obtained under the gel structure (not for an isolated filament). Some investigators have measured the fluorescence depolarization for DNA intercalated with ethidium bromide. Thomas et al.[18] obtained the torsional rigidity of DNA by the fluorescence depolarization method as $\alpha = 3.8 \times 10^{-12}$ dyn cm and $C = 1.29 \times 10^{-19}$ dyn cm^2, assuming that the helix axis is immobile (i.e., $F_n(t) = 1.0$) while Millar et al.[19] reported that $C = 1.43 \times 10^{-19}$ dyn cm^2. Hurley et al.[32] also obtained a similar value, $C = 1.5 \times 10^{-19}$ dyn cm^2 by the measurement of electron paramagnetic resonance. Shibata et al.[27] reanalyzed the data of Thomas to check the tumbling correlation function of Barkley and Zimm and obtained a larger value $\alpha = 7.2 \times 10^{-12}$ dyn cm and $C = 2.4 \times 10^{-19}$ dyn cm^2. Yoshizaki et al.[33] analyzed the data of Millar et al. with their original theory (the discrete helical wormlike chain model) and obtained an even larger value $C = (3.2\text{–}4.4) \times 10^{-19}$ dyn cm^2. In the latter analysis, the agreement between theory and experiment is not as good as that of the Barkley–Zimm theory employed by Millar et al. However, one cannot say which value is reasonable at the present time. The experiments of the kinetic rates of ligation[34,35] seem to support the latter value. The kinetic ligation data yield $\alpha = 8.7 \times 10^{-12}$ dyn cm and $C = 3.0 \times 10^{-19}$ dyn cm^2. Shimada and Yamakawa[36] also analyzed the ligase kinetics data by the theory for cyclization probability and topoisomer distribution based on the helical wormlike chain model and found that $C = (2.4\text{–}3.0) \times 10^{-19}$ dyn cm^2. The above inconsistency in the torsional rigidity from different experimental sources may be due to the difference in the amplitude of the bending of DNA in each experimental condition. The bending deformation of a ligated chain is larger than that of a linear chain. Hence, the apparent torsional rigidity may be different.

The torsional rigidity for the stereocomplex of PMMA was obtained in the same manner of analysis as that of Thomas et al.; namely, the intermediate zone formula was used for the twisting correlation function, on the assumption that the internal correlation function is time independent and that the helix axis is immobile. Therefore, it is reasonable to compare the value of the torsional rigidity of the stereocomplex with that of DNA by Thomas et al. We can recognize that the value of α of the stereocomplex is much larger than that of DNA: 2.4×10^{-10} dyn cm for the stereocomplex and 3.8×10^{-12} dyn cm for DNA. Even the value of C of the stereocomplex is larger by 1 order than that of DNA: 6.0×10^{-18} dyn cm^2 for the stereocomplex and 1.29×10^{-19} dyn cm^2 for DNA. These results may reflect the difference in the chemical structure between the stereocomplex and DNA; i.e., the number of interacting points per unit contour length is larger for the stereocomplex than that for DNA. Therefore, DNA has a large degree of freedom to cope with torsional deformations compared with the stereocomplex.

However, the torsional rigidity of the stereocomplex may also be due to the restriction of the torsional motion by

the cross-linking points under the gel structure. It is necessary to estimate the intrinsic torsional rigidity of the stereocomplex under no influence of such gel structure for more detailed comparison with the DNA data. Careful selection of the conditions for the preparation of sample solutions has to be made to avoid the gelation. These points are currently under investigation.

V. Conclusions

Fluorescence depolarization measurements revealed that the stereocomplex formation of i-PMMA and s-PMMA occurs at the ratio isotactic/syndiotactic = 1/2 in dilute toluene solution. We found that the formula of the autocorrelation function for the torsion dynamics of stiff polymer chains can explain the present data of $r(t)$ of the stereocomplex fairly well. This supports the idea of the double-stranded helical structure of the stereocomplex of PMMA, although another idea of the "extended structure" has been proposed.[37] From time-resolved fluorescence depolarization data, we estimated the torsional rigidity under the gel structure to be $\alpha = 2.4 \times 10^{-10}$ dyn cm and $C = 6.0 \times 10^{-18}$ dyn cm^2 at 25 °C. Both α and C are much larger than those of DNA. Thus, the PMMA stereocomplex under the gel structure is more rigid against torsional deformations than DNA. However, such an estimation may contain some uncertainty due to the hydrodynamic evaluation of the friction factor, γ. To solve this problem, other low-frequency experiments, which allow independent determination of the friction factor, would be required.

Acknowledgment. We are indebted to Dr. M. Uchida whose doctoral study at Kyoto University was incorporated in this work. Present work was supported by a Grant-in-Aid for Scientific Research (No. 62470094) from the Ministry of Education.

Registry No. (i-PMMA)(s-PMMA) (complex), 79616-50-5.

References and Notes

(1) Fox, T. G.; Garrett, B. S.; Goode, W. E.; Gratch, S.; Kincaid, J. F.; Spell, A.; Stroupe, J. D. *J. Am. Chem. Soc.* **1958**, *80*, 1768.
(2) Liquori, A. M.; Anzuino, G.; Coiro, V. M.; D'Alagni, M.; de Santis, P.; Savino, M. *Nature (London)* **1965**, *206*, 358.
(3) Watanabe, W. H.; Ryan, C. F.; Fleischer, P. C., Jr.; Garrett, B. S. *J. Phys. Chem.* **1961**, *65*, 896. Ryan, C. F.; Fleischer, P. C., Jr. *Ibid.* **1965**, *69*, 3384.
(4) Vorenkamp, E. J.; Bosscher, F.; Challa, G. *Polymer* **1979**, *20*, 59.
(5) Bosscher, F.; Keekstra, D.; Challa, G. *Polymer* **1981**, *22*, 124.
(6) Spěváček, J.; Schneider, B. *Makromol. Chem.* **1974**, *175*, 2939; **1975**, *176*, 729; *Colloid Polym. Sci.* **1980**, *258*, 621.
(7) Bosscher, F.; ten Brinke, G.; Challa, G. *Macromolecules* **1982**, *15*, 1442.
(8) ten Brinke, G.; Schomaker, E.; Challa, G. *Macromolecules* **1985**, *18*, 1925. Schomaker, E.; ten Brinke, G.; Challa, G. *Ibid.* **1985**, *18*, 1930.
(9) Miyamoto, T.; Inagaki, H. *Polym. J.* **1970**, *1*, 46.
(10) Yau, H.; Stupp, S. I. *J. Polym. Sci., Polym. Chem. Ed.* **1985**, *23*, 813.
(11) Allen, P. E. M.; Host, D. M.; Truong, V. T.; Williams, D. R. G. *Eur. Polym. J.* **1983**, *19*, 923.
(12) Chen, H.-L.; Morawetz, H. *Eur. Polym. J.* **1983**, *19*, 923.
(13) Bednář, B.; Morawetz, H.; Shafer, J. A. *Macromolecules* **1984**, *17*, 1634. Bednář, B.; Li, Z.; Huang, Y.; Chang, L.-C. P.; Morawetz, H. *Ibid.* **1985**, *18*, 1829.
(14) Anufrieva, E. V.; Pautov, V. O.; Papisov, I. M.; Kabanov, V. A. *Dokl. Akad. Nauk SSSR* **1977**, *232*, 1096.
(15) Uchida, M. Doctoral Thesis, Kyoto University, 1977.
(16) Barkley, M. D.; Zimm, B. H. *J. Chem. Phys.* **1979**, *70*, 2991.
(17) Allison, S. A.; Schurr, J. M. *Chem. Phys.* **1979**, *41*, 35.
(18) Thomas, J. C.; Allison, S. A.; Appellof, C. J.; Schurr, J. M. *Biophys. Chem.* **1980**, *12*, 177.
(19) Millar, D. P.; Robbins, R. J.; Zewail, A. H. *Proc. Natl. Acad. Sci. U.S.A.* **1980**, *77*, 5593; *J. Chem. Phys.* **1981**, *74*, 4200; **1982**, *76*, 2080.
(20) Elias, J. G.; Eden, D. *Macromolecules* **1981**, *14*, 410.
(21) Hargerman, P. J. *Biopolymers* **1981**, *20*, 1503.
(22) Hogan, M.; Wang, J.; Austin, R. M.; Monitto, C.; Hershkowitz, S. *Proc. Natl. Acad. Sci. U.S.A.* **1982**, *79*, 3518.
(23) Sasaki, T.; Yamamoto, M.; Nishijima, Y. *Macromolecules* **1988**, *21*, 610.
(24) Schurr, J. M. *Chem. Phys.* **1984**, *84*, 71.
(25) Yamakawa, H.; Fujii, M. *J. Chem. Phys.* **1976**, *64*, 5222.
(26) Yamakawa, H.; Shimada, J. *J. Chem. Phys.* **1979**, *70*, 609.
(27) Shibata, J. H.; Fujimoto, B. S.; Schurr, J. M. *Biopolymers* **1985**, *24*, 1909.
(28) Hatada, K.; Ute, K.; Tanaka, K.; Okamoto, Y.; Kitayama, T. *Polym. J.* **1986**, *18*, 1037.
(29) Wahl, Ph. *Biophys. Chem.* **1979**, *10*, 91.
(30) Vorenkamp, E. J.; Challa, G. *Polymer* **1981**, *22*, 1705.
(31) Perrin, F. *J. Phys. Radium* **1936**, *7*, 1.
(32) Hurley, I.; Osei-Gyimah, P.; Archer, S.; Scholes, C. P.; Lerman, L. S. *Biochemistry* **1982**, *21*, 4999.
(33) Yoshizaki, T.; Fujii, M.; Yamakawa, H. *J. Chem. Phys.* **1985**, *82*, 1003.
(34) Shore, D.; Baldwin, R. L. *J. Mol. Biol.* **1983**, *170*, 983.
(35) Horowitz, D. S.; Wang, J. C. *J. Mol. Biol.* **1984**, *173*, 75.
(36) Shimada, J.; Yamakawa, H. *Macromolecules* **1984**, *17*, 689.
(37) Dybal, J.; Štokr, J.; Schneider, B. *Polymer* **1983**, *24*, 971.